Biochimica et Biophysica Acta 1784 (2008) 1865–1872

Contents lists available at ScienceDirect

Biochimica et Biophysica Acta

journal homepage: www.elsevier.com/locate/bbapap

Cold adaptation of enzymes: Structural, kinetic and microcalorimetric characterizations of an aminopeptidase from the Arctic psychrophile *Colwellia psychrerythraea* and of human leukotriene A_4 hydrolase

Adrienne L. Huston [a,1], Jesper Z. Haeggström [b], Georges Feller [a,*]

[a] *Laboratory of Biochemistry, University of Liège, B-4000 Liège-Sart Tilman, Belgium*
[b] *Department of Medical Biochemistry and Biophysics, Karolinska Instituet, S-17177 Stockholm, Sweden*

ARTICLE INFO

Article history:
Received 24 April 2008
Received in revised form 30 May 2008
Accepted 3 June 2008
Available online 13 June 2008

Keywords:
Psychrophile
Cold-active enzyme
Aminopeptidase
Colwellia psychrerythraea
Leukotriene A_4 hydrolase

ABSTRACT

The relationships between structure, activity, stability and flexibility of a cold-adapted aminopeptidase produced by a psychrophilic marine bacterium have been investigated in comparison with a mesophilic structural and functional human homolog. Differential scanning calorimetry, fluorescence monitoring of thermal- and guanidine hydrochloride-induced unfolding and fluorescence quenching were used to show that the cold-adapted enzyme is characterized by a high activity at low temperatures, a low structural stability versus thermal and chemical denaturants and a greater structural permeability to a quenching agent relative to the mesophilic homolog. These findings support the hypothesis that cold-adapted enzymes maintain their activity at low temperatures as a result of increased global or local structural flexibility, which results in low stability. Analysis of the thermodynamic parameters of irreversible thermal unfolding suggests that entropy-driven factors are responsible for the fast unfolding rate of the cold-adapted aminopeptidase. A reduced number of proline residues, a lower degree of hydrophobic residue burial and a decreased surface accessibility of charged residues may be responsible for this effect. On the other hand, the reduction in enthalpy-driven interactions is the primary determinant of the weak conformational stability.

1. Introduction

Life on Earth has successfully colonized diverse environments considered extreme. Recent research has suggested that microorganisms are able to maintain their metabolic function at temperatures ranging from −39 °C in polar environments [1] to temperatures in excess of 100 °C in hydrothermal vents [2,3]. The microorganisms that survive and grow at these temperature extremes, termed thermally-adapted extremophiles, have adopted a variety of adaptive strategies to maintain activity and metabolic function despite challenging conditions. These strategies include synthesis of unique compounds such as cold- and heat-shock proteins [4,5], molecular chaperones [6], compatible solutes [7] and structural modifications leading to the maintenance of membrane fluidity [8], to name a few.

In addition to adaptations at the cellular level, a key adaptive strategy of extremophiles is the modification of enzyme kinetics, allowing the maintenance of sufficient reaction rates at thermal extremes. To maintain function, proteins must strike a balance of structural rigidity and flexibility in their respective environments. Rigidity is needed to ensure correct active site geometry for substrate and ligand binding, as well as to avoid denaturation, while flexibility is needed to enable accommodation of substrates and appropriate rates of catalysis [9,10]. While enzymes in low-temperature environments must contend with exponential decreases in chemical reaction rates and increasing structural compactness that can limit the conformational movement necessary for catalysis [11], enzymes in high-temperature environments must withstand thermal energies that lead to irreversible denaturation and chemical degradation. Therefore, a key question in the adaptation of organisms to different temperatures is, how do homologous enzymes maintain their function under extreme and divergent conditions?

To investigate the structural basis of enzymatic adaptation to different temperatures, numerous comparative studies on homologous proteins from mesophilic and thermophilic sources and more recently, from psychrophilic sources have been performed. The cold-active enzymes produced by psychrophiles derived from perennially-cold habitats have been found to be characterized by high catalytic efficiency at low temperatures and low structural stability relative to enzymes from meso- and thermophilic sources [12]. Current theory suggests that in order to maintain molecular movement necessary for catalysis at low temperatures, cold-active enzymes must possess

Abbreviations: ColAP, *Colwellia psychrerythraea* aminopeptidase; LTA4H, human leukotriene A_4 hydrolase; DSC, differential scanning calorimetry

* Corresponding author. Laboratory of Biochemistry, Institute of Chemistry B6a, B-4000 Liège-Sart Tilman, Belgium. Tel.: +32 4 366 33 43; fax: +32 4 366 33 64.
E-mail address: gfeller@ulg.ac.be (G. Feller).
[1] Present address: American Association for the Advancement of Science (AAAS), 1200 New York Avenue, NW, Washington, DC 20005, USA.

1570-9639/$ – see front matter © 2008 Elsevier B.V. All rights reserved.
doi:10.1016/j.bbapap.2008.06.002

enhanced flexibility in certain areas (e.g., catalytic site or hinge regions necessary for catalysis) of their protein structure, which also reduces their stability against thermal and denaturing reagents. The primary modifications implicated in the increased flexibility of cold-active enzymes are a general decrease in stabilizing weak interactions, such as salt bridges or hydrogen bonds, in the strength of the hydrophobic effect and in rigidifying structural factors such as proline residues. At present, thermal adaptation appears to be achieved by a combination of unique alterations for each enzyme investigated rather than a general universal strategy. Therefore, despite great fundamental and biotechnological interest [13], the structural determinants enabling maintenance of enzymatic activity and stability at different temperatures remain unclear. Further investigations of the structural features, thermodynamics of unfolding and conformational plasticity of enzymes obtained from different thermal environments are needed to address this issue.

In this paper we investigated the determinants of thermal adaptation in the case of M1 aminopeptidases. We directly compared the thermal and chemical stabilities, temperature dependence of activity and conformational flexibility of a cold-active aminopeptidase (ColAP) from the Arctic psychrophile *Colwellia psychrerythraea* 34H [14] with that of its mesophilic human homolog leukotriene A_4 hydrolase (LTA4H) involved in inflammation processes. The latter is a bifunctional zinc metalloenzyme which integrates aminopeptidase activity with a sophisticated epoxide hydrolase activity in a common active center [15]. LTA4H is a well-characterized enzyme for which the three-dimensional structure has been determined [16]. It was chosen as the mesophilic reference in this study because it resembles ColAP in terms of peptide substrate preferences, and it displays close conservation of the amino acid sequence and perfect conservation of amino acids involved in catalytic activity. ColAP is predicted to exhibit a similar folded structure consisting of three domains that together create a cleft forming the catalytic zinc site. The results presented here are the first of their kind for cold-active aminopeptidases, revealing relationships between activity, stability and flexibility in these enzymes.

2. Materials and methods

2.1. Three-dimensional modeling and analysis

Marine psychrophile *C. psychrerythraea* 34H was isolated from Greenland continental shelf sediment samples and characterized [17]. The *colap* gene encoding for the cold-active extracellular aminopeptidase was identified and sequenced as previously described [14]. Due to the high sequence similarity with ColAP relative to other proteins with known structures, the crystal structure of LTA4H [16] was chosen as a template for initial construction of a three-dimensional (3D) model of ColAP. Subsequent to construction of the initial comparative model, a structure prediction was performed by de novo methods [18]. Template selection, 3D modeling, and structural analysis were performed by using RAMP software available at the protein modeling server http://protinfo.compbio.washington.edu. Ionic interactions were determined by using cut-off distances of 4.0 Å between interacting groups. The solvent-accessible surface area was determined with a probe radius of 2.0 Å.

2.2. Cloning of colap

Genomic DNA was extracted from a batch culture of *C. psychrerythraea* 34H using the Promega wizard genomic DNA purification kit. The *colap* gene, including its signal sequence, was PCR-amplified using $Vent_R$ Thermopol Polymerase (New England Biolabs), with the sense primer (5′-TAAAATCATATGAAACATTTTTCAAAACTTTGC-3′) containing an NdeI site (underlined) and the antisense primer (5′-GATATTCTCGAG**TTA**TTTCAATACACCGTC-3′) containing an XhoI site (underlined) and the stop codon (bold). The PCR product was cloned into the PCR-Script Amp SK(+) cloning vector (Stratagene), excised with NdeI and XhoI and ligated into the pET22b(+) cloning vector (Novagen). The resulting recombinant plasmid was transformed into *Escherichia coli* BL21 (DE3) cells (Stratagene).

2.3. Production and purification of recombinant ColAP and LTA4H

Single colonies of the *E. coli* BL21 (DE3) cells transformed with the vector carrying the *colap* gene were used to inoculate 25 ml of an overnight culture of LB containing 200 μg ml^{-1} ampicillin at 18 °C. Five-ml aliquots were centrifuged at 5000 ×*g* for 10 min at 4 °C, and the pellets were resuspended in 250 ml of Terrific broth (12 g l^{-1} Bacto tryptone (Difco), 24 g l^{-1} yeast extract (Difco), 4 ml l^{-1} glycerol, 12.54 g l^{-1} K_2HPO_4, 2.31 g l^{-1} KH_2PO_4, pH 7.2) containing 200 mg ml^{-1} ampicillin in a 3-l flask. The cultures were incubated at 18 °C and 250 rpm until an absorbance at 550 nm reached 3–4. Expression of the enzymes was induced with 0.1 mM isopropyl-1-thio-β-galactopyranoside. Following a further 16-h incubation at 18 °C, the cells were harvested by centrifugation at 10,000 ×*g* for 30 min at 4 °C, resuspended in Buffer A (20 mM PIPES pH 6.75), disrupted in a prechilled high-pressure cell disrupter (Constant Systems) at 28 kpsi, centrifuged at 30,000 ×*g* for 30 min at 4 °C, and dialyzed against Buffer A overnight. The dialysate was then subjected to Q-Sepharose High Performance (75-ml bed volume; Amersham Pharmacia) chromatography using a linear gradient of Buffer A to Buffer A+350 mM NaCl over 12 bed volumes at 5 ml min^{-1}. Active fractions were pooled and further purified on a Hydroxyapatite column (75-ml bed volume; Bio-Rad) using a linear gradient from 10 mM Na_2HPO_4 pH 7.2 to 300 mM Na_2HPO_4 pH 6.8 over 12 bed volumes at 5 ml min^{-1}. Finally, active fractions were pooled and purified on a Mono-Q column (5-ml bed volume; Amersham Pharmacia) using a linear gradient of Buffer A to Buffer A+350 mM NaCl over 45 bed volumes at 1 ml min^{-1}. The Q-Sepharose and Mono-Q chromatography steps were performed at 4 °C, while the Hydroxyapatite chromatography was performed at room temperature due to precipitation of Na_2HPO_4 at low temperatures. The N-terminal amino acid sequence of the recombinant enzyme was determined by automated Edman degradation using a pulsed-liquid-phase protein sequencer Procise 494 (Applied Biosystems). The purified mesophilic homolog LTA4H was produced and purified as described [19].

2.4. Aminopeptidase assays and activity characterization

Immediately before all activity and biophysical characterizations, enzyme aliquots were centrifuged at 16,000 ×*g* for 10 min to remove any precipitated protein, and the resulting supernatant was used for subsequent characterization. Aminopeptidase activity was determined in 20 mM PIPES (pH 7.2), 400 mM NaCl using L-alanine-4-nitroanilide hydrochloride substrate in a thermostatted Uvikon 860 spectrophotometer (Kontron). The reaction was followed by monitoring the linear release of *p*-nitroaniline at 410 nm [20] over a period of 20 s. Concentration of the product was determined using an extinction coefficient of 8480 M^{-1} cm^{-1}. Kinetic constants for recombinant ColAP and LTA4H were determined at various temperatures from a series of initial rates at different substrate concentrations over the range of 0.1 to 50 mM. The thermodependence of activity was determined by performing assays using 10 μg ml^{-1} enzyme at various temperatures ranging from 3 to 60 °C in the presence of 10 and 20 mM substrate for ColAP and LTA4H, respectively. Protein concentrations were determined with the Coomassie Protein Assay Reagent (Pierce) using BSA as a standard, and by absorbance at 280 nm.

2.5. Leukotriene hydrolase activity assay

Epoxide hydrolase activity was assayed as described previously [21]. Briefly, 4 μg of protein was diluted into 100 μl of 25 mM Tris buffer, pH 7.8 containing 40 μM of leukotriene A_4 (5*S*-*trans*-5,6-oxido-

7,9-*trans*-11,14-*cis*-eicosatetraenoic acid). Reactions were performed for 10 s at 10, 15, 20, 25 and 30 °C. Activity was terminated by adding 200 µl methanol. The samples were further diluted with 100 µl water and a defined amount of the internal standard prostaglandin B_2 was added prior to HPLC analysis.

2.6. Unfolding recorded by intrinsic fluorescence

Fluorescence of ColAP and LTA4H was measured on an SML-AMINCO Model 8100 spectrofluorimeter (Spectronic Instruments) at excitation and emission wavelengths of 280 nm (2-nm band pass) and 330 nm (4-nm band pass), respectively. Protein samples were prepared in 20 mM MOPS, 100 mM NaCl pH 7.2 buffer at a concentration of 25 µg ml^{-1}. Heat-induced unfolding was performed at a scan rate of 2 °C min^{-1} using a programmed Lauda RE306 water bath. Data were normalized using the pre- and post-transition baseline slopes as described previously [22]. Scans were also performed in the presence of 2.5 mM L-arginine to reduce protein aggregation.

2.7. Differential scanning calorimetry

DSC was performed with a Microcal VP-DSC apparatus using the Observer software package (Version 7) for data acquisition, analysis and deconvolution. Samples were dialyzed overnight against 20 mM MOPS, 100 mM NaCl pH 7.2. Prior to DSC analysis, a non-detergent sulfobetaine 3-(1-pyridinio)-1-propanesulfonate was added at a concentration of 500 mM to decrease the effects of heat-induced protein aggregation [23]. A final protein concentration of 0.8 mg ml^{-1} was used. The rate constant for irreversible thermal unfolding (k_{denat}) was calculated as follows [24]:

$$k_{denat} = v\mathrm{Cp}/(\Delta H_{cal} - Q)$$

where v represents the scan rate (K min^{-1}), Cp the excess heat capacity at a given temperature, ΔH_{cal}, the total heat of the unfolding process and Q the heat evolved at a given temperature.

2.8. Calculation of thermodynamic parameters

The rate constants determined (k_{cat}, k_{denat}) were used to calculate the energy of activation (E_a) according to the Arrhenius equation and the thermodynamic parameters of activation were determined as described [25]:

$$\Delta G^{\#} = RT \times (\ln k_B T/h - \ln k)$$

$$\Delta H^{\#} = E_a - RT$$

$$T\Delta S^{\#} = (\Delta H^{\#} - \Delta G^{\#})$$

where k_B is the Boltzmann constant (1.38×10^{-23} J K^{-1}), h the Planck's constant (6.63×10^{-34} J s) and k (s^{-1}) is the rate constant at temperature T (K).

2.9. Guanidine hydrochloride unfolding

Approximately 25 µg ml^{-1} protein samples in 20 mM MOPS, 100 mM NaCl pH 7.2 were incubated overnight at 18 °C in defined guanidine hydrochloride (GdnHCl) concentrations (0–6.5 M) and protein unfolding was monitored by intrinsic fluorescence analysis. The pH was checked to ensure a constant value throughout the transition and denaturant concentrations were verified by refractive index measurements [22] using a R5000 hand refractometer from Atago. Relative fluorescence was determined on an SML-AMINCO Model 8100 spectrofluorimeter (Spectronic Instruments) at an excitation wavelength of 280 nm (2-nm band pass) and emission spectra were recorded from 300–420 nm (4-nm band pass). The intensity-weighted average emission wavelength [26] was calculated as follows:

$$(\lambda) = \sum \lambda_i F_i / \sum F_i$$

where λ_i and F_i represent the wavelengths measured and the corresponding emission intensities, respectively.

The influence of guanidine hydrochloride on activity was determined by measuring enzyme activity in the presence of varying concentrations of denaturant after overnight incubation in the same concentration. Reversibility of unfolding was determined by diluting denatured protein samples 20-fold in 20 mM MOPS, 100 mM NaCl pH 7.2 and measuring residual activity after a 44-h incubation at 18 °C. For activity measurements, samples diluted in the MOPS buffers were further diluted 4-fold into 20 mM PIPES, 400 mM NaCl pH 7.2 buffer immediately before assaying.

2.10. Dynamic fluorescence quenching

The acrylamide-induced quenching of intrinsic fluorescence of ColAP and LTA4H was measured on an SML-AMINCO Model 8100 spectrofluorimeter (Spectronic Instruments) at an excitation wavelength of 280 nm (1-nm band pass) and an emission wavelength of 330 nm (2-nm band pass). Protein samples were prepared in 20 mM MOPS, 100 mM NaCl pH 7.2 buffer at a concentration of 50 µg ml^{-1}. Aliquots of a 1.2 M acrylamide stock solution were consecutively added to 1 ml protein solution in regular intervals to increase the acrylamide concentration by 5 mM increments. The Stern–Volmer quenching constants K_{SV} were calculated according to the following equation [27]:

$$F_0/F = 1 + K_{SV}[Q]$$

where F and F_0 are the fluorescence intensity in the presence and absence of molar concentration of the quencher Q, respectively. The intrinsic protein fluorescence F was corrected for the acrylamide inner filter effect f, as defined by:

$$f = 10^{-\varepsilon[Q]/2}$$

using an extinction coefficient ε for acrylamide at 280 nm of 4.3 M^{-1} cm^{-1}.

3. Results

3.1. Sequence analysis and protein modeling

General results of multiple-sequence alignment between ColAP and LTA4H have been described previously [14]. Briefly, a 33% amino acid identity and a 57% amino acid similarity were determined between ColAP and LTA4H. Sequence alignment revealed perfect conservation of amino acids involved in substrate binding, zinc binding and aminopeptidase activity (Supplementary Fig. 1). Furthermore, biocomputational sequence analyses revealed amino acid identities distributed throughout the entire ColAP sequence that correspond well to secondary structural elements in LTA4H. In our current comparative analysis of the sequences and structures of ColAP and LTA4H, we focused on features hypothesized to affect the structural flexibility associated with low-temperature enzyme activity. In ColAP, the overall number of proline residues is reduced relative to LTA4H (Table 1). Biocomputation of the complete amino acid sequence using the Protparam tool indicated a higher potential solubility and solvent interaction potential of ColAP relative to LTA4H, as shown by a low grand average of hydropathy, GRAVY [28], and p*I*. There did not appear to be a significant reduction in arginine residues in ColAP (22 versus 23 in LTA4H), as has been observed in previous cold-active enzymes, which are capable of forming multiple salt bridges and H bonds. By contrast, modeling analysis suggested that ColAP has fewer ion pairs than LTA4H (15 versus 25), which leads to a decrease in the number of intrinsic stabilizing bonds.

Table 1
Summary of structural parameters possibly involved in thermal adaptation of ColAP and LTA4H

	ColAP	LTA4H
Proline content	25	35
% nonpolar residues of total	43.8	42.6
% polar residues of total	32.8	32.1
% charged residues of total	23.4	25.3
GRAVY index	−0.34	−0.26
Isoelectric point (p*I*)	5.25	5.80
Ion pairs	15	25

While there appeared to be no significant differences in the overall content of hydrophobic versus polar and charged residues, differential partitioning of the amino acid groups between the solvent-accessible and buried fractions of the structures was observed. In ColAP, a greater proportion of the accessible surface is comprised of hydrophobic and polar side chains, while a smaller proportion is comprised of charged side chains relative to LTA4H (Table 2). These trends are reflected by the accessibility and burial percentages of the amino acid groups. For example, in ColAP, 6.9% of the hydrophobic residues are fully surface accessible, while 43.8% are buried, compared with 0.8 and 49.4% for accessible and buried hydrophobic residues in LTA4H, respectively. Overall, these results indicate a lower degree of hydrophobic and uncharged residue burial and decreased surface accessibility of charged residues in ColAP relative to LTA4H. This trend was also observed in the catalytic cavity of both enzymes. Using data from the crystal structure of LTA4H in complex with the inhibitor bestatin [16], a high degree of conservation was observed between residues forming the catalytic cavities of both enzymes. Only 3 substitutions occurred: two replacements of tyrosine (Tyr 267 and 378, LTA4H numbering) with phenylalanine and the substitution Val 292 for leucine in ColAP.

3.2. Production and purification of ColAP

The production and purification procedures resulted in ~74 mg l^{-1} of pure ColAP with a recovery of ~22%. Purity was determined by both standard and overloaded SDS-PAGE (12% gels) indicating a single and homogeneous band with a molecular weight of ~70 kDa (68,593.5 Da calculated). Purity was further ascertained by N-terminal sequencing, which resulted in a single sequence HEGAT that was consistent with the predicted cleavage site of the signal peptide sequence. These results indicate that the signal peptide sequence was correctly cleaved and processed by *E. coli* BL21 (DE3).

3.3. Thermodependence of activity

The thermodependence of activity of ColAP and LTA4H is shown in Fig. 1A. It can be observed that ColAP exhibits a shift of maximal activity to lower temperatures of 10 °C relative to LTA4H (Table 3). ColAP exhibited significantly higher reaction rates than LTA4H over the entire temperature range investigated, before denaturation (maximal activities corresponded to 120 s^{-1} and 17 s^{-1} for ColAP and LTA4H, respectively). Analysis of the thermodynamic activation parameters at 10 °C (Fig. 1A, inset and Table 4) indicated that ColAP has a lower temperature dependence of activity resulting in a lower E_a and $\Delta H^{\#}$ when compared to LTA4H. ColAP did not exhibit epoxide hydrolase activity under the assay conditions described (data not shown) as has been previously observed with other M1 aminopeptidases, precluding comparative activity analysis with the epoxide hydrolase activity of LTA4H.

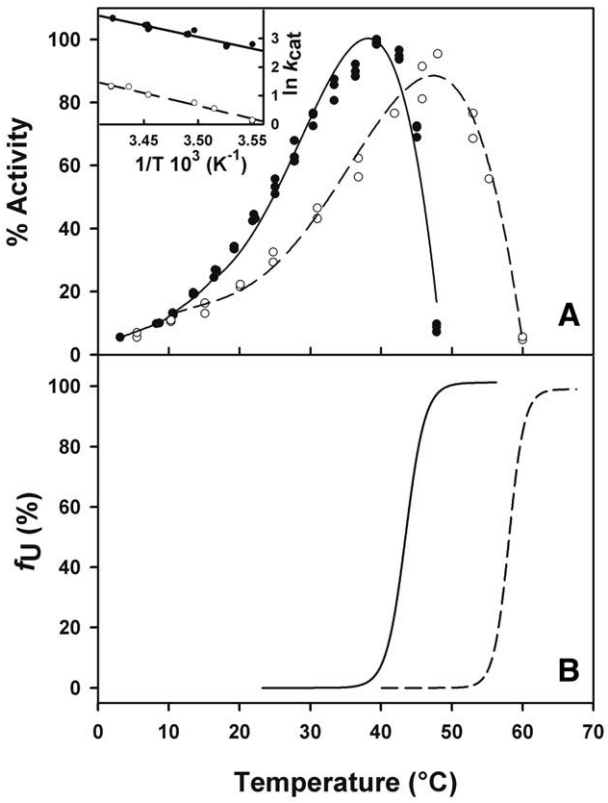

Fig. 1. Thermodependence of activity (A) inset; Arrhenius plot for activity, and denaturation as recorded by fluorescence emission (B) for the cold-adapted aminopeptidase ColAP (solid line, solid circles) and human LTA4H (dashed line, open circles).

3.4. Thermal stability

Heat-induced conformational unfolding recorded by fluorescence emission indicated that the T_m values for ColAP is 15 °C lower than that of LTA4H in MOPS buffer (Fig. 1B, Table 3). In the presence of 2.5 mM L-arginine, an additive previously reported to suppress protein aggregation during thermal unfolding studies [29], the T_m value of ColAP was increased by 3 °C (Table 3). By contrast, the T_m of

Table 2
Composition of the surface accessible and buried regions of ColAP and LTA4H

	ColAP	LTA4H
Surface accessibility (Å^2)		
Accessible surface	26,471	23,919
Surface of nonpolar residues	7503 (28.3%)	5401 (22.6%)
Surface of polar residues	7858 (29.7%)	7018 (29.3%)
Surface of charged residues	11,110 (42%)	11,500 (48.1%)
Accessibility percentages (100% surface accessible)		
% nonpolar residues of total	6.9	0.8
% polar residues of total	11.8	6.6
% charged residues of total	32.34	42.75
Burial percentages (<10% surface accessible)		
% nonpolar residues of total	43.8	49.4
% polar residues of total	31.8	34.6
% charged residues of total	10.1	7.8

Table 3
The apparent optimal temperature for activity and thermodynamic parameters of heat-induced unfolding of ColAP and LTA4H

Enzyme	Activity	Fluorescence emission		Differential scanning calorimetry		
	T_{opt}	Arginine	T_m	Scan rate	T_m	ΔH_{cal}
	°C	mM	°C	K min^{-1}	°C	kJ mol^{-1}
ColAP	39	0.0	43.5	0.5	45.5	241
		2.5	46.5	1.0	46.7	264
				1.5	47.4	291
LTA4H	49	0.0	58.5	0.5	57.2	598
		2.5	57.5	1.0	58.2	678
				1.5	59.1	733

Table 4
Thermodynamic parameters for activity and irreversible thermal unfolding for ColAP and LTA4H

	Enzyme	T	k	E_a	$\Delta G^{\#}$	$\Delta H^{\#}$	$T\Delta S^{\#}$
		°C	s^{-1}	kJ mol^{-1}	kJ mol^{-1}	kJ mol^{-1}	kJ mol^{-1}
Activity	ColAP	10	15.8	68	63	66	3
(k_{cat})	LTA4H	10	1.9	75	68	73	5
Irreversible	ColAP	46	1.1×10^{-2}	737	90	735	645
unfolding	LTA4H	46	1.0×10^{-7}	622	121	620	499
(k_{denat})	ColAP	45	2.0×10^{-3}	737	94	734	640
	LTA4H	56	2.0×10^{-3}	622	98	619	521

LTA4H decreased by 1 °C in the presence of 2.5 mM arginine. In all conditions, the unfolding of both enzymes was irreversible, as evidenced by a lack of transition observed while rescanning denatured samples after cooling. Thermal unfolding of ColAP and LTA4H was also monitored by differential scanning calorimetry (DSC) in the presence of a non-detergent sulfobetaine, 3-(1-pyridinio)-1-propanesulfonate (NDSB) to avoid heat-induced aggregation [23]. As seen in Fig. 2 and Table 3, conformational unfolding (as determined by T_m and ΔH_{cal}) was scan rate-dependent, indicating that the thermal denaturation of these proteins is under kinetic control. The lack of heat absorption effects upon rescanning of denatured samples furthermore indicated that conformational unfolding was irreversible (data not shown). The kinetically-driven unfolding of both enzymes was therefore analyzed according to a two-state irreversible denaturation model [24]. The stability of ColAP was low relative to LTA4H, with average apparent T_m values of 46.5 and 58.2 °C, and average ΔH_{cal} values of 265 and 670 kJ mol^{-1}, respectively. These T_m values are in agreement with those recorded by intrinsic fluorescence. The thermodynamic parameters of activation for the denaturation process (Table 4) have been calculated both at an identical temperature (46 °C) and at an identical unfolding rate (2.0×10^{-3} s^{-1}). At the same temperature, the denaturation rate k_{denat} was five orders of magnitude higher for the relatively unstable ColAP and correspondingly, the energy barrier for unfolding ($\Delta G^{\#}$) was lower relative to LTA4H. Interestingly, the $\Delta H^{\#}$ and $T\Delta S^{\#}$ contributions were all higher for ColAP, but resulted in a lower $\Delta G^{\#}$ value. Comparison of these data suggests that the weak kinetic stability of ColAP is entropy-driven.

3.5. Chemical stability

The stability of ColAP and LTA4H was investigated by GdnHCl-induced unfolding as monitored by intrinsic fluorescence. As shown in Fig. 3A, both enzymes appeared to unfold via multiple transitions, suggesting the presence of denaturation intermediates. For both enzymes, unfolding occurred at distinct concentrations of GdnHCl, with ColAP exhibiting transitions at lower denaturant concentrations relative to LTA4H. Fig. 3B illustrates the percentage of original activity retained after incubation in varying concentrations of denaturant. While the activity initially increased ~2-fold for LTA4H at low denaturant concentrations, the loss of activity for both enzymes corresponded directly to the first transition of unfolding. Analysis of the reversibility of unfolding as monitored by recovery of activity (Fig. 3C) shows that the first unfolding transition corresponded to a complete loss of reversibility for both enzymes. However, while LTA4H unfolding remained irreversible at higher denaturant concentrations, ColAP regained a significant level of activity (up to ~72%) at denaturant concentrations corresponding to and above the second unfolding transition. Aggregates were observed (by absorption at 450 nm) at concentrations corresponding to unfolding transitions for both enzymes. For ColAP, aggregates

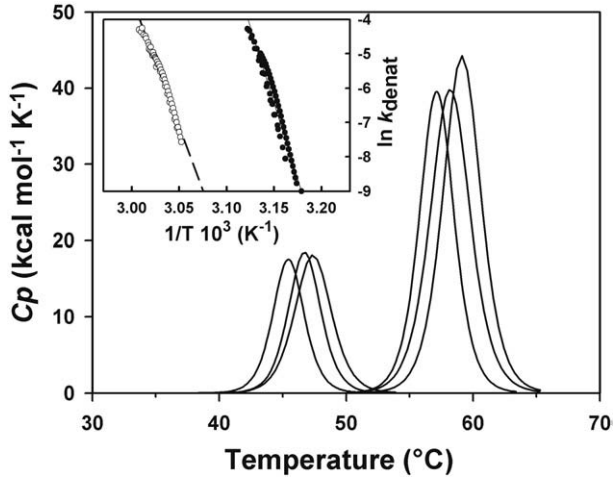

Fig. 2. Thermal unfolding as monitored by DSC at scan rates of 0.5, 1.0, and 1.5 K min^{-1} for ColAP (left curves) and human LTA4H (right curves). Inset: Arrhenius plot for the irreversible denaturation of ColAP (solid line, solid circles) and LTA4H (dashed line, open circles).

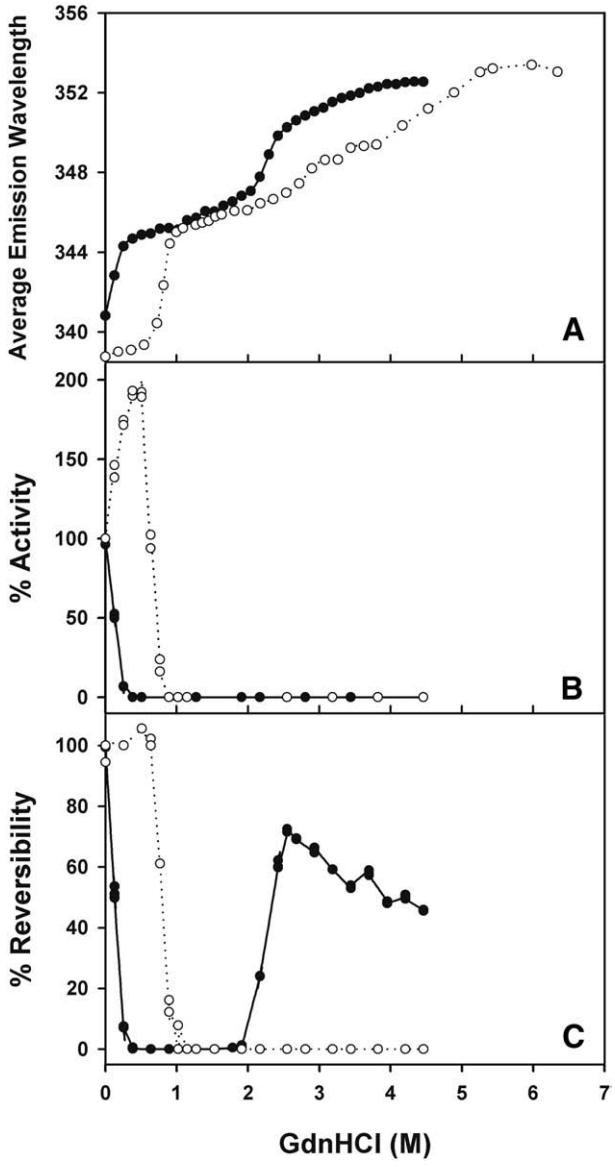

Fig. 3. Guanidine hydrochloride unfolding of the cold-adapted aminopeptidase ColAP (solid line, solid circles) and human LTA4H (dotted line, open circles). (A) Unfolding monitored by the average emission wavelength. (B) Dependence of enzyme activity on guanidine hydrochloride concentration. (C) Reversibility of guanidine hydrochloride unfolding by recovery of activity after 20-fold dilution.

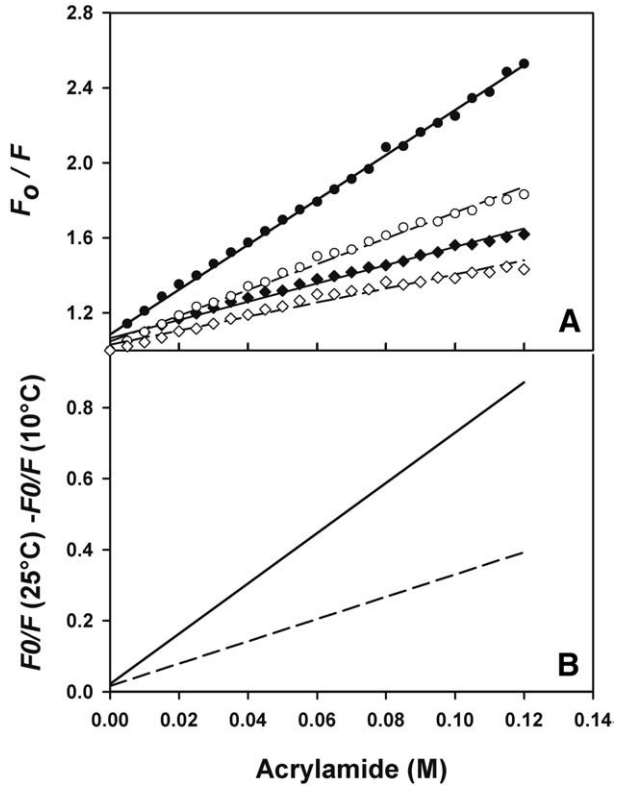

Fig. 4. Stern–Volmer plots of fluorescence quenching by acrylamide of ColAP (solid lines, solid symbols) and human LTA4H (dashed lines, open symbols). The upper panel shows the fluorescence (F_0/F) ratios at 10 °C (diamonds) and 25 °C (circles). The lower panel shows the variation of the fluorescence ratios obtained by subtracting the regression lines (25 °C–10 °C).

were observed only at denaturant concentrations below the second unfolding transition, while LTA4H aggregates were observed at all concentrations above the first unfolding transition. Thus, irreversibility of unfolding coincided with the presence of aggregates in GdnHCl for both enzymes.

3.6. Fluorescence quenching

The structural permeability of the enzymes was investigated by dynamic fluorescence quenching of aromatic residues (dominated by tryptophan) by acrylamide. The Stern–Volmer plots for ColAP and LTA4H at 10 and 25 °C (Fig. 4A), suggest a higher accessibility of fluorophore residues in ColAP, particularly at the higher temperature incubation. Because the absolute values of the Stern–Volmer quenching constant (K_{SV}) can only be compared if the number and location of aromatic residues are identical in both structures, the difference between the slopes of the Stern–Volmer plots at 10 and 25 °C was used to illustrate the difference in structural permeability of both enzymes with an increase in temperature (Fig. 4B). The higher slope for ColAP indicates a greater accessibility of aromatic residues relative to LTA4H, indicating a greater permeability of the enzyme structure to the small quencher molecule, at temperatures where the native and active states prevails.

4. Discussion

In this study we have investigated the relationship between structure, activity, stability and flexibility of an aminopeptidase (ColAP) produced by a psychrophilic bacterium in comparison with a mesophilic structural and functional human homolog (LTA4H).

4.1. Activity properties of ColAP

The psychrophilic enzyme displays a shift in optimal aminopeptidase activity to lower temperatures by 10 °C and an increased retention of activity at low and moderate temperatures relative to LTA4H. Furthermore, at all temperatures measured, the specific aminopeptidase activity of ColAP is significantly higher than for LTA4H by at least a factor of 7. The latter property is considered as the main physiological adaptation to cold at the enzyme level [30]. In the case of ColAP, Table 4 reveals that a significant contribution to this high activity at low temperatures is provided by the low activation enthalpy $\Delta H^{\#}$ that primarily reflects a weaker temperature dependence of the activity. Accordingly, when the reaction temperature is reduced, the activity of ColAP is less reduced than that of human LTA4H. This low activation enthalpy also suggests that fewer enthalpy-driven interactions have to be disrupted to reach the activated state in ColAP and, interestingly, the substitutions noted in its active site (Tyr 267 and Tyr 378 into Phe in ColAP) tend to decrease the potential for hydrogen bonding with other moieties.

The psychrophilic ColAP does not exhibit LTA_4 hydrolase activity at any of the temperatures tested. This is consistent with previous studies showing that despite exhibiting conservation of most putative catalytic residues and overall three-dimensional structure, M1 aminopeptidases derived from a variety of sources lack epoxide hydrolase activity [31]. In this respect, ColAP represents an interesting case study as all residues involved in leukotriene A_4 hydrolase activity in human LTA4H are strictly conserved in the bacterial enzyme. The three substitutions detected in the ColAP active site (Tyr267Phe, Tyr378Phe and Val292Leu, LTA4H to ColAP substitutions) are therefore suitable targets for mutagenesis studies aimed at deciphering the molecular origin of this complex activity of the human enzyme. LTA_4 hydrolase activity has also been shown to depend upon a specific binding conformation of the substrate LTA_4 [16,32]. The two Tyr to Phe substitutions may act to disrupt the proper binding of the LTA_4 substrate by resulting in a smaller binding cavity in addition to removal of the Tyr 267 hydroxyl group, thought to be important in determining the configuration of LTA4H binding [16]. Furthermore, inspection of residues corresponding to the binding pocket of LTA4H reveals two noticeable non-conservative substitutions (Phe362Asp and Ile372Arg). These introduced charges may preclude proper binding of the LTA_4 substrate aliphatic chain in ColAP.

Fluorescence emission studies reveal that ColAP displays a shift in structural unfolding to lower temperatures by 15 °C, indicating a greatly reduced stability relative to LTA4H. Previous studies have observed that the activity loss of cold-active proteins occurs at temperatures farther below the onset of structural unfolding relative to mesophilic and thermophilic enzymes, whose activity loss has been found to correspond closely to losses in native protein conformation [30]. These results have suggested that the active sites of cold-active enzymes have a pronounced lability when compared with other structural regions and were the basis for the concept of localized increases in conformational flexibility during cold adaptation [33,34]. In this study however, comparison of the activity with conformational unfolding as observed by fluorescence emission (Fig. 1) reveals that thermal inactivation of ColAP closely corresponds to the beginning of the unfolding transition. This suggests that changes in native protein conformation are the primary determinant for loss of activity in ColAP, rather than temperature-induced perturbation of the active site. It should be noted that the cold-active enzymes previously analyzed in this manner did not contain a metal binding site in their catalytic cavities [35–37]. By contrast, in ColAP, the presence of a Zn^{2+} ion may act to stabilize the active site relative to other structural areas.

4.2. Origin of the weak conformational stability of ColAP

A deeper understanding of the factors resulting in the weak stability of ColAP can be obtained from the microcalorimetric and thermodynamic analyses of protein unfolding. The calorimetric thermal unfolding studies reveal that both monomeric, multi-domain enzymes unfold into one calorimetric domain, with ColAP exhibiting lower melting temperatures when compared to LTA4H (Fig. 2). ColAP also exhibits significantly decreased microcalorimetric enthalpy values, ΔH_{cal}, indicating that fewer enthalpy-driven interactions are disrupted during thermal unfolding (Table 3). These results indicate that enthalpic destabilization contributes to the weak structural stability of the cold-active enzyme relative to its human homolog. This is corroborated by the modeling studies predicting fewer ion pairs in ColAP. The thermal unfolding of both enzymes is irreversible, as is often found for proteins larger than 20 kDa [38]. Slower scan rates yielded lower T_m values, indicating a kinetically-driven unfolding process. Analysis of the microcalorimetric data in the formalism of the transition-state theory yields information regarding the differences in the stabilizing forces for the two enzymes. As shown in Table 4, thermal unfolding of ColAP proceeds with a lower free energy of activation ($\Delta G^{\#}$) relative to LTA4H, that is directly related to the larger denaturation rate at a given temperature, and corresponds to a low kinetic barrier for unfolding of the psychrophilic enzyme. Referring to the classical Gibbs–Helmholtz relation:

$$\Delta G^{\#} = \Delta H^{\#} - T\Delta S^{\#}$$

it can be seen in Table 4 that this low kinetic barrier arises from larger enthalpic and entropic contributions when compared with LTA4H. Furthermore, in the absence of the entropic term $T\Delta S^{\#}$, the kinetic stability of ColAP would be higher than that of the human homolog. This is not the case, as a result of the large entropic contribution, and one can therefore conclude that the weak kinetic stability of ColAP is entropy-driven. Thus, the large activation enthalpy, $\Delta H^{\#}$, basically reflects the temperature dependence of unfolding: for a given increase in temperature, the increase of the unfolding rate of ColAP is much higher than for LTA4H. This is in agreement with the low number of enthalpy-driven interactions disrupted during unfolding as evidenced by the ΔH_{cal} values (Table 3).

On the other hand, the large entropic contribution suggests that the transition state of ColAP unfolding is more disordered than that of LTA4H. Although macroscopic interpretations of entropy should be taken with caution, results of comparative structural studies provide insights into the possible origin of this contribution in the psychrophilic aminopeptidase. The homology-based model of ColAP structure indicates that the molecule has a lower proportion of buried hydrophobic residues while exposing a higher proportion of hydrophobic residues to the solvent relative to LTA4H (Table 2). These structural changes may explain the observed entropy-driven destabilizing factor; the entropy loss due to reorganization of water molecules around nonpolar side chains exposed upon unfolding will be lower for ColAP, thereby weakening the hydrophobic effect on protein folding. Structural analysis also indicates that ColAP has fewer proline residues than LTA4H. In folded as well as in denatured proteins, proline residues restrict motions of the peptide backbone due to rotational constraints around the N–Cα bond and reducing backbone flexibility and local mobility of the chain [39]. The lower proportion of prolines in ColAP may also act to increase the conformational entropy of the unfolded state thus serving as a destabilizing factor with regard to the native state [40,41].

In agreement with thermal unfolding studies, GdnHCl-induced unfolding curves indicate that the stability of the proteins is directly related to the thermal regime of the producing organism. Indeed, ColAP displays a low stability when exposed to chemical denaturants, as suggested by unfolding transitions and loss of activity at lower guanidine hydrochloride (GdnHCl) concentrations relative to LTA4H (Fig. 3). While the unfolding of LTA4H was aggregate-prone and irreversible at all GdnHCl concentrations above the first unfolding transition, ColAP unfolding was aggregate-prone and irreversible only at intermediate GdnHCl concentrations. At higher denaturant concentrations corresponding to the second unfolding transition, ColAP unfolded via a reversible pathway with no observable aggregates (Fig. 3C). Thus, at intermediate GdnHCl concentrations, ColAP may have become incorporated into aggregates before complete unfolding took place. Interestingly, this unusual behavior has also been observed for a psychrophilic xylanase [35]. This suggests that the structural adaptations of psychrophilic enzymes may be responsible for a specific GdnHCl-induced unfolding pathway that remains to be properly understood. The effect of GdnHCl on the activity of both enzymes (Fig. 3B) provides additional insights into the activity–stability relationships in these aminopeptidases. While the activity loss of ColAP occurred immediately upon addition of GdnHCl, LTA4H activity initially increased up to ~2-fold at concentrations below the first unfolding transition. Enzyme activation by moderate denaturant concentrations has been frequently reported and was generally interpreted as resulting from the relaxation of structural constraints, improving active site flexibility, and allowing full expression of the catalytic power [42–44]. In this respect, one can therefore propose that the psychrophilic ColAP is already in this relaxed and unstable state and consequently moderate denaturant concentrations lead to fast unfolding and activity loss.

Determination of molecular flexibility requires the definition of the types and amplitudes of atomic motions as well as a timescale for these motions. In this respect, dynamic fluorescence quenching used during this study, usefully averages most of these parameters into a single signal. As shown in Fig. 4, the structure of the psychrophilic ColAP has an improved propensity to be penetrated by a small quencher molecule when compared to human LTA4H. The increase of this permeability index with temperature is also much higher for ColAP. This reveals a less compact conformation undergoing frequent micro-unfolding events of the native state and larger native state fluctuations for the cold-adapted protein.

In conclusion, our results support the “corresponding states” hypothesis [45] postulating that enzyme homologs exhibit comparable flexibilities to perform catalysis at their physiologically-relevant temperatures, as well as the proposed role of structural flexibility in enzymatic activity and stability with respect to thermal adaptation [9]. It is well known that many different strategies may be utilized to achieve thermal adaptation of proteins. Mutagenesis studies with ColAP are currently underway to further explore in detail the structural features enabling the maintenance of activity at low temperatures.

Acknowledgments

We thank N. Gerardin for her expert technical assistance, R. Samudrala for the 3D modeling and A. Hoyoux, T. Collins, S. D'Amico, J.-C. Marx, C. Beauvois and C. Gerday for their assistance and fruitful discussions. This work was supported by a National Science Foundation Post-Doctoral Fellowship awarded to ALH, by grants from the Fonds National de la Recherche Scientifique, Belgium to GF and from the Swedish Research Council (10350) to JZH.

Appendix A. Supplementary data

Supplementary data associated with this article can be found, in the online version, at doi:10.1016/j.bbapap.2008.06.002.

References

[1] N.S. Panikov, P.W. Flanagan, W.C. Oechel, M.A. Mastepanov, T.R. Christensen, Microbial activity in soils frozen to below −39 °C, Soil Biol. Biochem. 38 (2006) 784–794.

[2] E. Blochl, R. Rachel, S. Burggraf, D. Hafenbradl, H.W. Jannasch, K.O. Stetter, *Pyrolobus fumarii*, gen. and sp. nov., represents a novel group of archaea, extending the upper temperature limit for life to 113 degrees C, Extremophiles 1 (1997) 14–21.

[3] K. Kashefi, D.R. Lovley, Extending the upper temperature limit for life, Science 301 (2003) 934.

[4] R. Cavicchioli, T. Thomas, P.M. Curmi, Cold stress response in Archaea, Extremophiles 4 (2000) 321–331.

[5] M. Ouhammouch, Transcriptional regulation in Archaea, Curr. Opin. Genet. Dev. 14 (2004) 133–138.

[6] K. Motohashi, Y. Watanabe, M. Yohda, M. Yoshida, Heat-inactivated proteins are rescued by the DnaK.J-GrpE set and ClpB chaperones, Proc. Natl. Acad. Sci. U. S. A. 96 (1999) 7184–7189.

[7] J.F. Carpenter, J.H. Crowe, The mechanism of cryoprotection of proteins by solutes, Cryobiology 25 (1988) 244–255.

[8] N.J. Russell, Molecular adaptations in psychrophilic bacteria: potential for biotechnological applications, Adv. Biochem. Eng. Biotechnol. 61 (1998) 1–21.

[9] P. Zavodszky, J. Kardos, Svingor, G.A. Petsko, Adjustment of conformational flexibility is a key event in the thermal adaptation of proteins, Proc. Natl. Acad. Sci. U. S. A. 95 (1998) 7406–74011.

[10] P.A. Fields, Protein function at thermal extremes: balancing stability and flexibility, Comp. Biochem. Physiol. A Mol. Integr. Physiol. 129 (2001) 417–431.

[11] B.F. Rasmussen, A.M. Stock, D. Ringe, G.A. Petsko, Crystalline ribonuclease A loses function below the dynamical transition at 220 K, Nature 357 (1992) 423–424.

[12] G. Feller, Molecular adaptations to cold in psychrophilic enzymes, Cell. Mol. Life Sci. 60 (2003) 648–662.

[13] A.L. Huston, Biotechnological aspects of cold-adapted enzymes, in: R. Margesin, F. Schinner, J.C. Marx, C. Gerday (Eds.), Psychrophiles: from Biodiversity to Biotechnology, Springer Verlag, Heidelberg, 2007, pp. 347–363.

[14] A.L. Huston, B. Methe, J.W. Deming, Purification, characterization, and sequencing of an extracellular cold-active aminopeptidase produced by marine psychrophile *Colwellia psychrerythraea* strain 34H, Appl. Environ. Microbiol. 70 (2004) 3321–3328.

[15] J.Z. Haeggstrom, Leukotriene A4 hydrolase/aminopeptidase, the gatekeeper of chemotactic leukotriene B4 biosynthesis, J. Biol. Chem. 279 (2004) 50639–50642.

[16] M.M. Thunnissen, P. Nordlund, J.Z. Haeggstrom, Crystal structure of human leukotriene A(4) hydrolase, a bifunctional enzyme in inflammation, Nat. Struct. Biol. 8 (2001) 131–135.

[17] A.L. Huston, B.B. Krieger-Brockett, J.W. Deming, Remarkably low temperature optima for extracellular enzyme activity from Arctic bacteria and sea ice, Environ. Microbiol. 2 (2000) 383–388.

[18] R. Samudrala, M. Levitt, A comprehensive analysis of 40 blind protein structure predictions, BMC Struct. Biol. 2 (2002) 3–18.

[19] M. Blomster, A. Wetterholm, M.J. Mueller, J.Z. Haeggstrom, Evidence for a catalytic role of tyrosine 383 in the peptidase reaction of leukotriene A4 hydrolase, Eur. J. Biochem. 231 (1995) 528–534.

[20] E.G. DelMar, C. Largman, J.W. Brodrick, M.C. Geokas, A sensitive new substrate for chymotrypsin, Anal. Biochem. 99 (1979) 316–320.

[21] P.C. Rudberg, F. Tholander, M.M. Thunnissen, J.Z. Haeggstrom, Leukotriene A4 hydrolase/aminopeptidase. Glutamate 271 is a catalytic residue with specific roles in two distinct enzyme mechanisms, J. Biol. Chem. 277 (2002) 1398–1404.

[22] C.N. Pace, Determination and analysis of urea and guanidine hydrochloride denaturation curves, Methods Enzymol. 131 (1986) 266–280.

[23] T. Collins, S. D'Amico, D. Georlette, J.C. Marx, A.L. Huston, G. Feller, A nondetergent sulfobetaine prevents protein aggregation in microcalorimetric studies, Anal. Biochem. 352 (2006) 299–301.

[24] J.M. Sanchez-Ruiz, J.L. Lopez-Lacomba, M. Cortijo, P.L. Mateo, Differential scanning calorimetry of the irreversible thermal denaturation of thermolysin, Biochemistry 27 (1988) 1648–1652.

[25] T. Lonhienne, C. Gerday, G. Feller, Psychrophilic enzymes: revisiting the thermodynamic parameters of activation may explain local flexibility, Biochim. Biophys. Acta 1543 (2000) 1–10.

[26] C.A. Royer, C.J. Mann, C.R. Matthews, Resolution of the fluorescence equilibrium unfolding profile of trp aporepressor using single tryptophan mutants, Protein Sci. 2 (1993) 1844–1852.

[27] J.R. Lakowicz, B.P. Maliwal, Oxygen quenching and fluorescence depolarization of tyrosine residues in proteins, J. Biol. Chem. 258 (1983) 4794–4801.

[28] J. Kyte, R.F. Doolittle, A simple method for displaying the hydropathic character of a protein, J. Mol. Biol. 157 (1982) 105–132.

[29] M. Ishibashi, K. Tsumoto, D. Ejima, T. Arakawa, M. Tokunaga, Characterization of arginine as a solvent additive: a halophilic enzyme as a model protein, Protein Pept. Lett. 12 (2005) 649–653.

[30] G. Feller, C. Gerday, Psychrophilic enzymes: hot topics in cold adaptation, Nat. Rev. Microbiol. 1 (2003) 200–208.

[31] J.Z. Haeggstrom, Structure, function, and regulation of leukotriene A4 hydrolase, Am. J. Respir. Crit. Care Med. 161 (2000) S25–S31.

[32] F. Tholander, F. Kull, E. Ohlson, J. Shafqat, M.M. Thunnissen, J.Z. Haeggstrom, Leukotriene A4 hydrolase, insights into the molecular evolution by homology modeling and mutational analysis of enzyme from *Saccharomyces cerevisiae*, J. Biol. Chem. 280 (2005) 33477–33486.

[33] P.A. Fields, G.N. Somero, Hot spots in cold adaptation: localized increases in conformational flexibility in lactate dehydrogenase A4 orthologs of Antarctic notothenioid fishes, Proc. Natl. Acad. Sci. U. S. A. 95 (1998) 11476–11481.

[34] B.M. Beadle, B.K. Shoichet, Structural bases of stability-function tradeoffs in enzymes, J. Mol. Biol. 321 (2002) 285–296.

[35] T. Collins, M.A. Meuwis, C. Gerday, G. Feller, Activity, stability and flexibility in glycosidases adapted to extreme thermal environments, J. Mol. Biol. 328 (2003) 419–428.

[36] S. D'Amico, J.C. Marx, C. Gerday, G. Feller, Activity–stability relationships in extremophilic enzymes, J. Biol. Chem. 278 (2003) 7891–7896.

[37] D. Georlette, B. Damien, V. Blaise, E. Depiereux, V.N. Uversky, C. Gerday, G. Feller, Structural and functional adaptations to extreme temperatures in psychrophilic, mesophilic, and thermophilic DNA ligases, J. Biol. Chem. 278 (2003) 37015–37023.

[38] P.L. Privalov, Stability of proteins. Proteins which do not present a single cooperative system, Adv. Protein Chem. 35 (1982) 1–104.

[39] B.W. Matthews, H. Nicholson, W.J. Becktel, Enhanced protein thermostability from site-directed mutations that decrease the entropy of unfolding, Proc. Natl. Acad. Sci. U. S. A. 84 (1987) 6663–6667.

[40] D.K. Eggers, J.S. Valentine, Molecular confinement influences protein structure and enhances thermal protein stability, Protein Sci. 10 (2001) 250–261.

[41] H.X. Zhou, Loops, linkages, rings, catenanes, cages, and crowders: entropy-based strategies for stabilizing proteins, Acc. Chem. Res. 37 (2004) 123–130.

[42] V. Rehaber, R. Jaenicke, Stability and reconstitution of D-glyceraldehyde-3-phosphate dehydrogenase from the hyperthermophilic eubacterium *Thermotoga maritima*, J. Biol. Chem. 267 (1992) 10999–11006.

[43] Y.X. Fan, M. Ju, J.M. Zhou, C.L. Tsou, Activation of chicken liver dihydrofolate reductase in concentrated urea solutions, Biochim. Biophys. Acta 1252 (1995) 151–157.

[44] D.S. Burdette, V.V. Tchernajencko, J.G. Zeikus, Effect of thermal and chemical denaturants on *Thermoanaerobacter ethanolicus* secondary-alcohol dehydrogenase stability and activity, Enzyme Microb. Technol. 27 (2000) 11–18.

[45] G.N. Somero, Proteins and temperature, Annu. Rev. Physiol. 57 (1995) 43–68.